environmental microbiology

Environmental Microbiology (2021) **23**(1), 499–511 doi:10.1111/1462-2920.15340

Adh4, an alcohol dehydrogenase controls alcohol formation within bacterial microcompartments in the acetogenic bacterium *Acetobacterium woodii*

Nilanjan Pal Chowdhury,† **Jimyung Moon**† **and Volker Müller***

Department of Molecular Microbiology and Bioenergetics, Institute of Molecular Biosciences, Johann Wolfgang Goethe University Frankfurt/Main, Frankfurt, Germany.

Summary

***Acetobacterium woodii* utilizes the Wood-Ljungdahl pathway for reductive synthesis of acetate from carbon dioxide. However, *A. woodii* can also perform non-acetogenic growth on 1,2-propanediol (1,2-PD) where instead of acetate, equal amounts of propionate and propanol are produced as metabolic end products. Metabolism of 1,2-PD occurs *via* encapsulated metabolic enzymes within large proteinaceous bodies called bacterial microcompartments. While the genome of *A. woodii* harbours 11 genes encoding putative alcohol dehydrogenases, the BMC-encapsulated propanol-generating alcohol dehydrogenase remains unidentified. Here, we show that Adh4 of *A. woodii* is the alcohol dehydrogenase required for propanol/ethanol formation within these microcompartments. It catalyses the NADH-dependent reduction of propionaldehyde or acetaldehyde to propanol or ethanol and primarily functions to recycle NADH within the BMC. Removal of *adh4* gene from the *A. woodii* genome resulted in slow growth on 1,2-PD and the mutant displayed reduced propanol and enhanced propionate formation as a metabolic end product. In sum, the data suggest that Adh4 is responsible for propanol formation within the BMC and is involved in redox balancing in the acetogen, *A. woodii*.**

Introduction

Acetogens are characterized by their ability to synthesize acetyl-CoA by the reduction of CO_2 by H_2 using the Wood-Ljungdahl pathway (Wood and Ljungdahl, 1991). While they can sustain their carbon demand solely from gaseous carbon (autotrophic growth), they can also utilize several other organic substrates for growth as sole carbon source like hexoses, pentoses, diols, alcohols, lactate, formate, glycine betaine and acetaldehyde (Drake *et al*., 1997; Müller, 2003; Schuchmann and Müller, 2016). Growth on either of these substrates leads to the formation of the common product, acetate (Ljungdahl, 1969; Ragsdale and Wood, 1985; Drake, 1994). However, some acetogens like *A. woodii* can also grow non-acetogenically, as for example, by dismutation of 1,2-propanediol (1,2-PD) to propionate and propanol (Schuchmann *et al*., 2015). Metabolism of 1,2-PD by *A. woodii* is thought to occur within specialized proteinaceous bacterial microcompartments encasing multiple metabolic enzymes responsible for catabolism of 1,2-PD. Bacterial microcompartments (BMCs) are a functionally unique group of proteinaceous 'organelles' that are used to compartmentalize specific metabolic module(s), which lead to the formation of toxic or volatile intermediates. While these BMCs are solely composed of selectively permeable shell proteins, the movement of substrates or intermediates in and out of the metabolic core is selectively controlled by restricting the outward diffusion of toxic intermediates from BMCs (Kerfeld *et al*., 2005; Sampson and Bobik, 2008; Chowdhury *et al*., 2014).

BMCs are assembled by mainly three type of shell proteins, BMC-H (hexamers), BMC-T (pseudohexamer) and BMC-P (pentamer) (Kerfeld *et al*., 2005; Klein *et al*., 2009), while the function of a particular BMC is designated by the specific signature enzymes encapsulated within the BMC core. Depending on the encapsulated enzymes, BMCs are classified in two main categories, anabolic (carboxysome) and catabolic (metabolosome) (Kerfeld *et al*., 2005; Axen *et al*., 2014). While carboxysomes are characterized by their signature enzymes like carbonic anhydrase and RubisCO (Shively *et al*., 1973; Shively *et al*., 2001), metabolosomes involved in catabolism of 1,2-PD or ethanolamine are characterized by the presence of a B_{12}-dependent diol

Received 22 October, 2020; revised 18 November, 2020; accepted 30 November, 2020. *For correspondence. E-mail vmueller@bio.uni-frankfurt.de; Tel. (+49) 69 7982 9507; Fax (+49) 69 7982 9306. †These authors contributed equally to this work.

dehydratase (PduCDE) (Toraya *et al*., 1979; Bobik *et al*., 1997) or B_{12}-dependent ethanolamine lyase (EutBC) (Blackwell and Turner, 1978; Kofoid *et al*., 1999) respectively. Metabolosomes functions to retain the toxic propionaldehyde or acetaldehyde generated by the respective signature enzymes, which is further disproportionated to corresponding alcohol and acyl-CoA by an alcohol dehydrogenase and an aldehyde dehydrogenase respectively. The generated acyl-CoA is then activated by an incoming phosphate to an acyl-phosphate by a phosphotransacetylase (PTAC) which is further dephosphorylated to generate ATP by substrate level phosphorylation (SLP) (Rondon and Escalante-Semerena, 1992; Havemann *et al*., 2002; Penrod and Roth, 2006).

Acetobacterium woodii also produce BMCs during growth on 1,2-PD (Schuchmann *et al*., 2015) where the substrate is first dehydrated to propionaldehyde by coenzyme B_{12}-dependent diol dehydratase (PduCDE). The generated propionaldehyde is then converted to propionate by a coenzyme A-dependent propionaldehyde dehydrogenase (PduP), phosphotransacylase and propionate kinase. In the parallel branch, another molecule of propionaldehyde is reduced to propanol by a putative alcohol dehydrogenase by the NADH generated by PduP (see Fig. 1B). The internal recycling of NAD^+ within the BMC lumen is achieved by two separate encapsulated enzymes working in tandem. In *A. woodii*, the genes responsible for BMC formation and also its internal enzymes are encoded in a 20-gene contiguous *pdu* gene cluster (Chowdhury *et al*., 2020). The *pdu* cluster consists of two genes for a two-component system (histidine kinase and response regulator), six genes encoding shell proteins (*pduABB'KNT*), five genes for 1,2-PD degradation (*pduCDELP*) and four accessory genes for enzyme reactivation (*pduOSGH*) (Schuchmann *et al*., 2015; Chowdhury *et al*., 2020). Interestingly, a comparison of the *pdu* gene cluster of *A. woodii* to that of *Salmonella enterica* (Bobik *et al*., 1999) revealed that several genes are missing in *A. woodii* (Fig. 1A). Among them, three genes for shell formation (*pduJMU*), one accessory gene for vitamin B12 synthesis (*pduX*), propionate kinase (*pduW*) and most importantly propanol dehydrogenase (*pduQ*). While *A. woodii* codes for an acetate kinase (*ackA*) that is located elsewhere in the genome, it harbours 11 genes encoding putative alcohol dehydrogenases (Poehlein *et al*., 2012). One of them, *adhE* (bifunctional alcohol dehydrogenase) is the key enzyme involved in ethanol and acetaldehyde metabolism and not produced during metabolism of 1,2-PD (Bertsch *et al*., 2016). Two genes are annotated as putative butanol dehydrogenase (*bdh1* and *bdh2*) and another as putative 1,2-propanediol dehydrogenase (*dhaT*), the remaining seven genes as alcohol dehydrogenase (*adh1-adh7*) (Bertsch *et al*., 2016). As the current model of 1,2-PD metabolism (Fig. 1B) describes NAD^+ recycling to occur within the BMC, it is imperative that at least one of the 10 alcohol dehydrogenases co-localizes with the PduP within the BMC and recycles the reducing cofactor NAD^+.

In our prior study, with enriched BMCs we have shown that the CoA-dependent propionaldehyde dehydrogenase enzyme, PduP, localizes within the BMC of *A. woodii* (Chowdhury *et al*., 2020). In this study, we show that Adh4 is the missing alcohol (propanol) dehydrogenase involved in 1,2-PD degradation by *A. woodii*. With heterologously over-produced enzyme, we characterize the enzymatic properties of Adh4 and with the help of *in vivo* pull-down experiments with histidine-tagged PduB we show that both PduP and Adh4 interacts with PduB and co-localizes within the BMC. To address the potential function of the propanol forming alcohol dehydrogenase (Adh4) in the reductive branch of 1,2-PD metabolism, we deleted the *adh4* gene in *A. woodii* and studied the phenotype of the mutant strain. The results presented here identified the missing propanol dehydrogenase to localize within the BMC and on the other hand, revealed a complex electron balancing within two metabolic modules of non-acetogenic and acetogenic growth of *A. woodii* on 1,2-PD.

Results

Expression analysis of putative alcohol dehydrogenase genes of A. woodii *during BMC forming conditions*

Our earlier studies have shown that BMCs are not only produced during growth on 1,2-PD but also during heterotrophic growth of *A. woodii* on ethanol (Bertsch *et al*., 2016), acetaldehyde (Trifunovic *et al*., 2020), 2,3-butanediol (2,3-BD) (Hess *et al*., 2015), ethylene glycol (Trifunović *et al*., 2016) or fructose (Schuchmann *et al*., 2015). During growth on many of these substrates, alcohol dehydrogenases apparently play an important role. While the *A. woodii* genome encodes 11 putative Adhs, only the bifunctional AdhE has been purified and characterized to be the key enzyme involved in ethanol and acetaldehyde metabolism of *A. woodii* (Bertsch *et al*., 2016; Trifunovic *et al*., 2020). However, during growth on either 1,2-PD or 2,3-BD, AdhE was not produced by *A. woodii*. This led us to question and investigate which of the other 10 Adhs localize within the BMC during metabolism of 1,2-PD. From our earlier study, semi-quantitative measurement of expression levels of the putative *adh* genes during growth on ethanol or fructose revealed apart from *adhE* elevated transcript abundance of *adh4*, *adh6* and *adh1* genes (Bertsch *et al*., 2016). Further, a transcriptomic analysis of

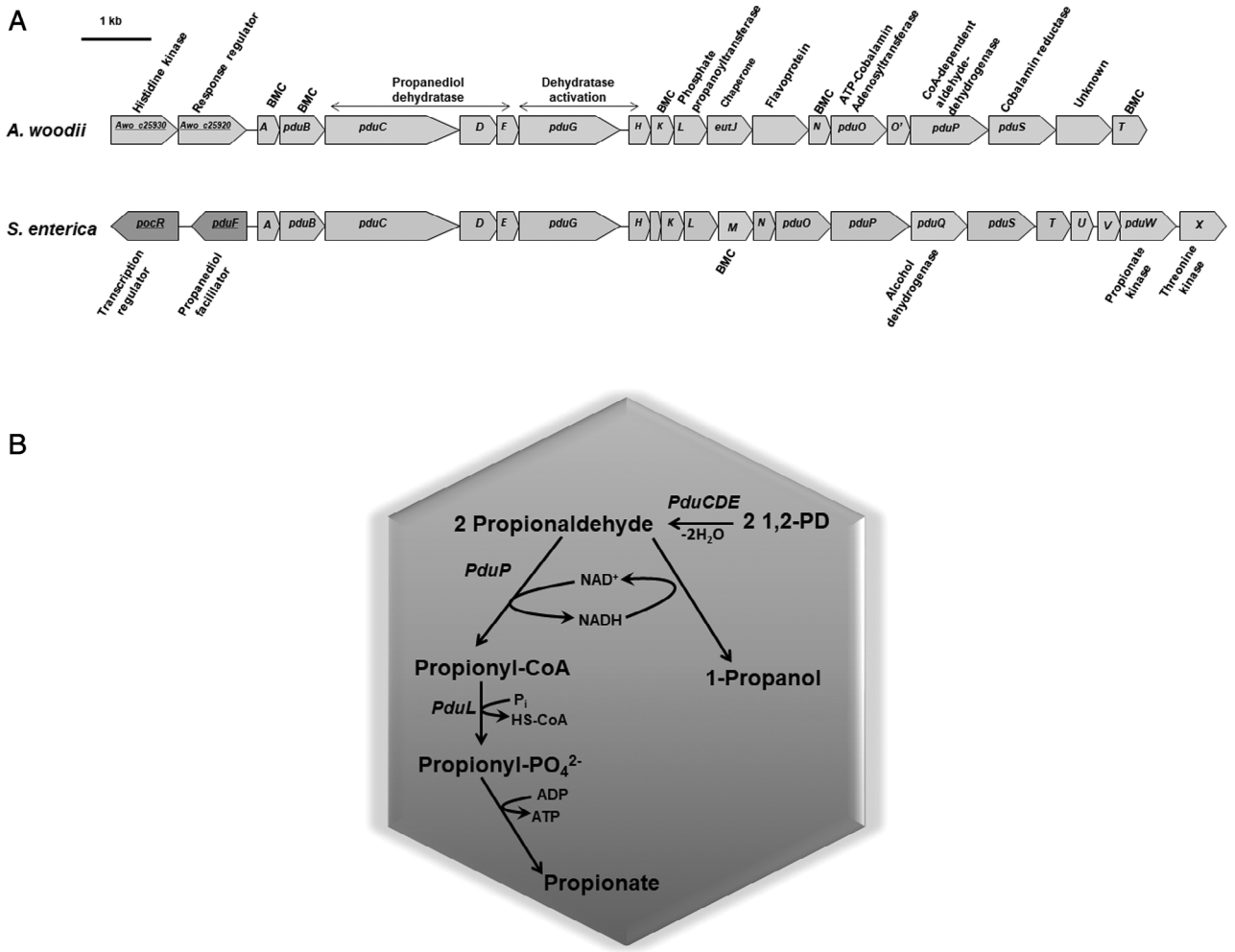

Fig. 1. Genetic organization of the *pdu* gene cluster in *A. woodii* and *S. enterica* (A) and model of 1,2-PD metabolism in *A. woodii*.
(A) The genes involved in 1,2-PD degradation and shell components of BMC in *A. woodii* (upper panel) and *S. enterica* (lower panel) are clustered in a single continuous locus. The 20 gene *pdu* cluster in *A. woodii* encodes five structural shell protein PduABKNT. In contrast to *S. enterica*, six genes, *pduM*, *pduQ*, *pduU*, *pduV*, *pduW* and *pduX*, are absent in *A. woodii*. Among them, *pduQ* encodes the signature enzyme propanol dehydrogenase.
(B) The propanediol-utilizing BMCs in *A. woodii* encapsulate three-signature enzymes, propanediol dehydratase (PduCDE), CoA-dependent aldehyde dehydrogenase (PduP) and an unidentified alcohol dehydrogenase. First, 1,2-PD is dehydrated by PduCDE to propionaldehyde, which is further disproportionated to propionyl-CoA by PduP or propanol by the unidentified alcohol dehydrogenase, while NAD^+/NADH is recycled by the disproportionation of propionaldehyde.

A. woodii cells grown on 1,2-PD also revealed that among all the *adhs* present in the genome, only these three *adhs* (*adh1*, *adh6* and *adh4*) were by far the most expressed (Chowdhury *et al*., 2020). To address which of these three putative alcohol dehydrogenases were differentially expressed during growth of *A. woodii* on 1,2-PD, 2,3-BD or ethylene glycol (BMC-forming conditions), we analysed mRNA levels of the representative *adh* genes during growth on these substrates. qRT-PCR analysis revealed very low levels of *adh1* transcripts during growth under BMC-forming conditions whereas up to 20 times higher transcript levels of *adh6* or *adh4* were obtained during growth on 2,3-BD and ethylene glycol or 1,2-PD. Expression of both *adh4* and *adh6* was highest during growth on 2,3-BD followed by 1,2-PD and ethylene glycol (Fig. 2B).

Adh4 and Adh6 shared only 33% identity to each other and around 35% identity to propanol dehydrogenase (PduQ) from *Salmonella enterica*. Both contains a putative N-terminal iron binding domain (Reid and Fewson, 1994), typical of bacterial oxygen-sensitive alcohol dehydrogenases. Interestingly, a closer look at the genetic organization of these two genes within the *A. woodii* genome revealed that *adh6* (Awo_c25410) is localized between two MFS_1 (major facilitator family) sugar transporter (Awo_c25420 and Awo_c25400)

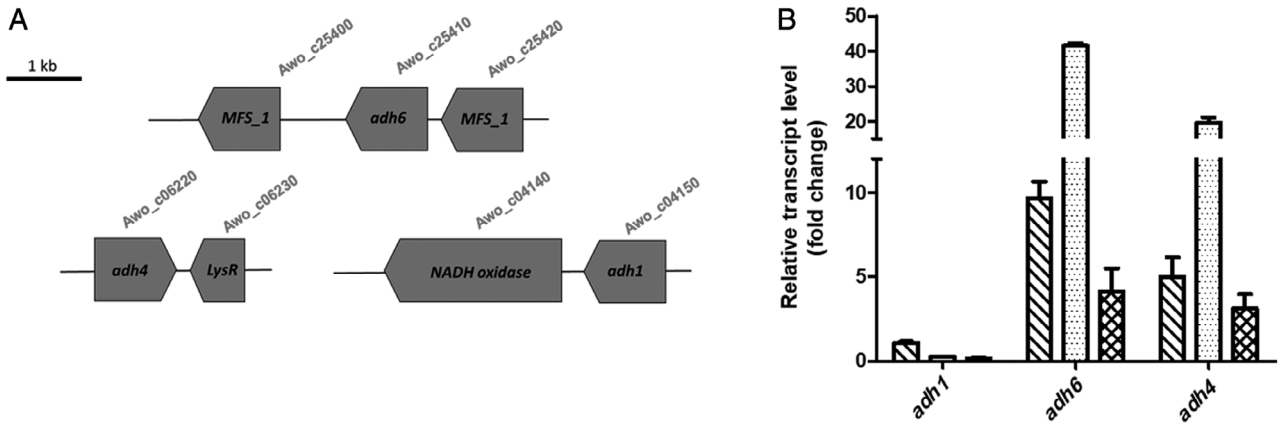

Fig. 2. Genetic organization (A) and expression of three different alcohol dehydrogenase genes (*adh1*, *adh4* and *adh6*) (B). Transcript levels of the three putative alcohol dehydrogenases during growth on three different substrates: 20 mM 2,3-BD (dots), 50 mM ethylene glycol (double cross) and 15 mM 1,2-PD (cross). Data plotted are from three independent mid exponential cultures.

genes, whereas *adh4* (Awo_c06220) localizes as a single gene with a downstream *LysR* family transcriptional regulator (Awo_c06230) (Fig. 2A).

Overproduction and purification of histidine tagged Adh4 and Adh6

Further, to analyse and identify the specific alcohol dehydrogenase involved in NAD^+ recycling within the BMC and generation of propanol from propionaldehyde, both *adh4* and *adh6* genes were cloned separately in the plasmid pET21a(+). A DNA sequence encoding a His-tag was inserted at the 3′-end of each gene and the plasmid was transformed into *Escherichia coli* BL21 (DE3). His_6-tagged Adh4 and Adh6 were produced in large amounts *via* a T7 expression system. Cell-free extract prepared from these recombinant strains was loaded on to a Ni-NTA column and histidine-tagged proteins were purified by an affinity chromatography. Both Adh4 (Fig. 3A) and Adh6 (Fig. 3B) with an expected size of ~40 kDa (as deduced from the respective amino acid sequence) were purified to a 95% homogeneity.

Enzymatic analysis of purified Adh4 and Adh6

To analyse the function of Adh4 and Adh6, NADH-dependent propionaldehyde reduction and NAD^+-dependent 1-propanol oxidation activities for both of these His_6-tagged enzymes (affinity purified) were tested under strict anoxic conditions. While Adh6 exhibited very low NADH oxidation with propionaldehyde, Adh4 rapidly oxidized NADH with propionaldehyde. Adh4 had about 150-fold higher propionaldehyde reductase activity than Adh6. The experimentally obtained propionaldehyde-reductase specific activity (V_{max}) for Adh4 was about 140.5 ± 6.5 μmol min^{-1} mg^{-1} with a K_m value of 50 ± 6 mM for propionaldehyde (Fig. 4). When propionaldehyde was replaced by butyraldehyde or acetaldehyde, the V_{max} was 153.4 ± 2 μmol min^{-1} mg^{-1} and 170.6 ± 1.7 μmol min^{-1} mg^{-1} respectively (Fig. S1). When butyraldehyde was replaced by isobutyraldehyde, V_{max} was only 10% of the optimum, 12.7 ± 0.5 μmol min^{-1} mg^{-1}. Oxidation of NADH was strictly propionaldehyde dependent and followed allosteric sigmoidal kinetics, the apparent K_m value for NADH was determined to be 0.27 mM. The pH and the temperature optima for Adh4 were at pH 7.0 and 30°C respectively. The activity of the enzyme rapidly decreased with either increasing pH of the assay buffer or temperature (Fig. S2), which is consistent with the pH and temperature preference of several other alcohol dehydrogenases (Reid and Fewson, 1994).

Adh4 also catalysed the reverse reaction, the oxidation of 1-propanol to propionaldehyde, which was strictly NAD^+ dependent. NAD^+ was reduced with 1-propanol with an activity of 0.63 ± 0.02 μmol min^{-1} mg^{-1} and the apparent K_m value for NAD^+ was determined to be 0.25 mM (Fig. S3). Surprisingly, while Adh4 exhibited bi-directional activity, Adh6 exhibited an extremely low propionaldehyde-reductase activity (V_{max} = 0.3 μmol min^{-1} mg^{-1}). While both the enzymes were purified under similar conditions, the activities of Adh4 and Adh6 are apparently different.

Adh4 is an integral component of intact BMCs

To determine the localization of Adh4, BMCs were enriched from *A. woodii* cells grown on 1,2-PD. The enriched BMCs were separated on a 12% SDS polyacrylamide gel and a protein fractionation pattern similar to earlier studies (Chowdhury *et al*., 2020) was obtained on staining the gel with Coomassie brilliant blue (Fig. 5). Since several proteins with expected molecular mass of

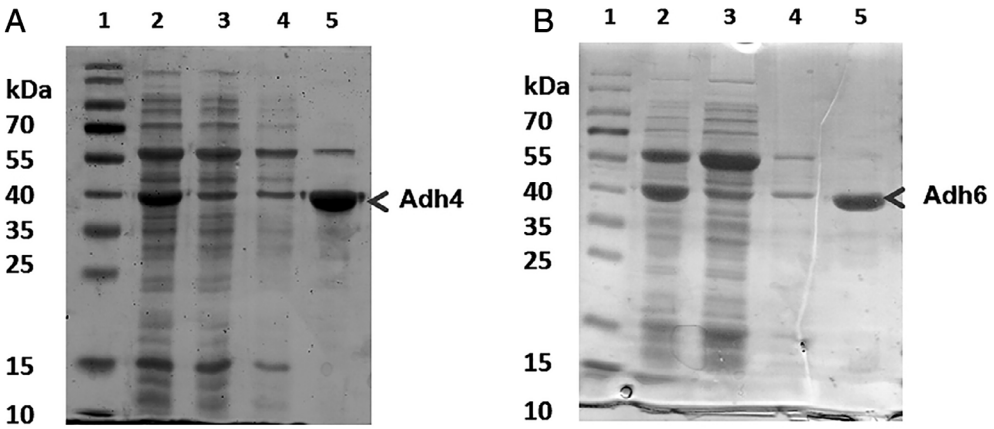

Fig. 3. Overproduction and purification of putative alcohol dehydrogenase Adh4 and Adh6. SDS-PAGE analysis of the purified Adh4-His_6 (A) and Adh6-His_6 (B) from *E. coli BL21*. Lane 1, protein standards; lane 2, cell-free extract; lane 3, flow through fraction; lane 4, wash fraction; lane 5, elution fraction. The proteins were separated on a 12% polyacrylamide gel and stained with Coomassie brilliant blue G250.

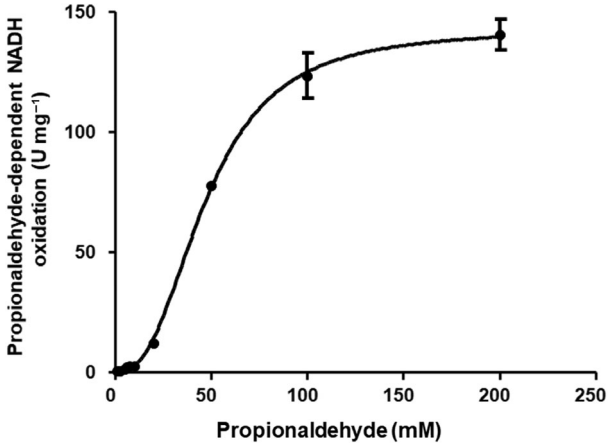

Fig. 4. Propionaldehyde dependence of Adh4 activity. The propionaldehyde dependent NADH oxidation was measured in an assay mixture containing 10 μg His_6-Adh4 in 50 mM Tris–HCl buffer (pH 7.5), 50 mM NaCl, 2 mM DTE, 4 μM resazurin and 250 μM NADH. Dependence of Adh4 activity on the concentration of propionaldehyde used in each assay was determined. The K_m and V_{max} values were calculated from non-linear regression using the GraphPad Prism program (version 5.01). Each data point is a mean ± SEM; n = 3 independent experiments.

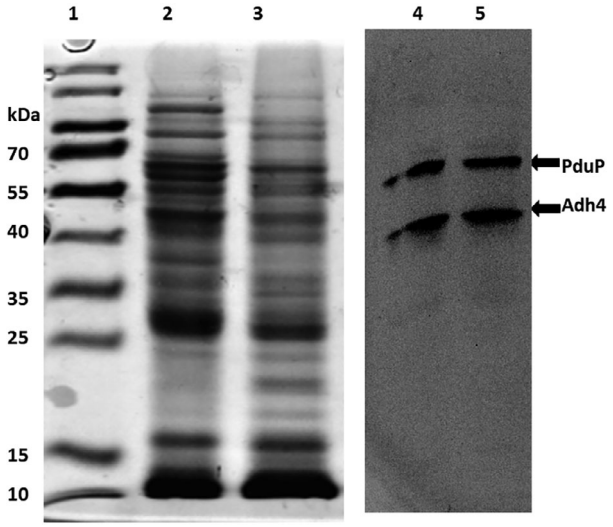

Fig. 5. SDS-PAGE of enriched BMCs and immunological determination of key proteins. BMCs from *A. woodii* cells (grown on 1,2-PD) were enriched as described earlier (Chowdhury *et al*., 2020) and 20 μg protein was applied to a 12% denaturing SDS-polyacrylamide gel. Lane 1, molecular mass standards; lane 2, sucrose cushion pellet; lane 3, 0.45 μm filtered pellet resuspension. The presence of PduP and Adh4 was determined immunologically in pellet fraction (4) and filtered resuspension of the pellet (5).

Adh4 (~41 kDa) were observed on the polyacrylamide gel, antibodies were raised against Adh4 (see Experimental procedures) for the purpose of immunoblotting experiments.

The presence of Adh4 was determined immunologically with anti-Adh4 antibodies. Indeed, the anti-Adh4 antibody reacted with only one protein that also fitted in size to Adh4. These results clearly confirmed the presence of Adh4 within the BMCs. Further, the presence of the internal protein (PduP) within the same protein enrichment was also analysed immunologically. As seen in Fig. 5, the enriched preparation contained both the encapsulated signature enzymes Adh4 and PduP together within the same BMC preparation. In our earlier report, we proved that BMCs purified in this method were intact and enclosed (Chowdhury *et al*., 2020). Hence, the results presented here show that indeed Adh4 localizes within the BMCs and is likely involved in NAD^+ recycling.

In vivo *pull-down assay using His6-tagged PduB*

To further confirm the observed internalization of Adh4 within the BMCs, potential binding interaction studies between the shell protein PduB and Adh4 were

performed. For this purpose, a strategy was developed where a DNA sequence encoding a His-tag was inserted at the 3′- end of the *pduB* and cloned into the pMTL82254 plasmid (Heap *et al*., 2007) containing the *pdu* promoter (see Materials and methods) and transformed into the wild type *A. woodii*. In our earlier study, we observed strong activation of the *pdu* promoter by 20 mM 2,3-BD (Chowdhury *et al*., 2020). Hence, transformed *A. woodii* cells were grown on 20 mM 2,3-BD as a sole carbon source and production of the His_6-PduB was auto-induced during growth on 2,3-BD. Cell-free extracts containing His_6-tagged PduB were prepared from the 2,3-BD grown cells and passed over a Ni-NTA affinity column. Low affinity binding proteins were washed out with buffers containing low imidazole concentrations (20 mM). His_6-PduB was then eluted from the column with 250 mM imidazole in the elution buffer. SDS-PAGE of the eluted His_6-PduB protein demonstrated that multiple proteins co-eluted with the major protein,PduB (Fig. 6A). Western blot analysis of the eluted protein with antibodies against PduB, PduT, PduP, PduC and Adh4 revealed that indeed PduB interacts with the outer shell protein PduT and also with the internal proteins PduC/PduP and Adh4 (Fig. 6B). Binding of PduB to Adh4 is consistent with the finding that Adh4 localizes within the BMCs and also further proves that Adh4 is an encapsulated protein that also interacts with the major shell protein, PduB.

Deletion of Adh4 causes delayed growth phenotype on 1,2-propanediol

As Adh4 was found associated with the BMCs and likely fulfils the essential function of NAD^+ recycling within the BMCs during growth on 1,2-PD, we aimed to delete the gene (Awo_06220) encoding Adh4 from the *A. woodii* genome, and study the phenotype of the mutant. The immediate downstream gene of *adh4* (Awo_06220) is a LysR-type regulator (Awo_06230) that was not modified to avoid hindrance to any other regulated processes (Fig. 2A). In order to create the a*dh4* deletion in *A. woodii*, a suicide plasmid pMTL84151_JM_dadh4 was generated, carrying approximately 1000 bp region (both upstream and downstream) flanking the *adh4* gene. The plasmid was integrated into the chromosome at one flanking region under antibiotic pressure (thiamphenicol) and subsequently, disintegration was forced by the presence of 5-fluoroorotate since the plasmid contained the *pyrE* cassette together with its promoter for production of a functional orotate phosphoribosyltransferase (Westphal *et al*., 2018). The mutants were isolated using fructose as a sole carbon source. The potential a*dh4* mutants were screened and verified using PCR and sequence analysis. The *adh4* mutant failed to grow on media containing 15 mM 1,2-PD as sole carbon source even after several attempts. Since *A. woodii* needs a longer adaptation for growth on 15 mM 1,2-PD, this may have caused the growth phenotype. In our earlier study, we reported when *A. woodii* cells grown on 100 mM formate to a stationary phase and then 15 mM 1,2-PD was added, a rapid growth on 1,2 PD was observed (Chowdhury *et al*., 2020). Both Δ*pyrE* and Δ*adh4* strains were grown on 100 mM formate as a sole carbon and energy source and on reaching the stationary phase (OD_{600} = 0.35), 15 mM 1,2-PD was added to the culture. Growth was monitored after addition of 1,2-PD and growth of Δ*adh4* strain was at least 54% slower than the Δ*pyrE* strain (doubling time of 9.6 ± 0.2 h versus 6.3 ± 0.3 h). The Δ*adh4* strain also grew to a much lower cell density compared to the Δ*pyrE* strain (OD_{600} of 0.60 versus 0.75) (Fig. 7). A similar observation of delayed growth phenotype and lower final optical density of a *pduQ* (propanol

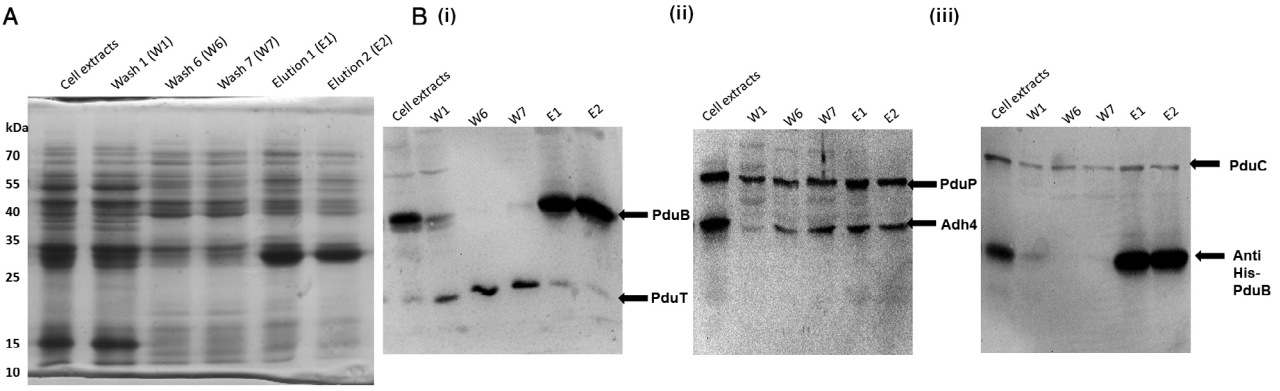

Fig. 6. His_6-PduB interacts with the internal core enzymes of BMC. SDS-PAGE monitoring of the purification process of the His_6-PduB from *A. woodii*. (A) After each purification step, 20 μg protein fractions was applied on to 12% polyacrylamide gel (Laemmli, 1970). Lane 1, cell-free extract of *A. woodii* producing His_6-PduB. Lane 2–4, wash fractions. Lane 5–6, elution fractions. (B) The presence of PduB and PduT (i), PduP and Adh4 (ii) and PduC and His_6-PduB (iii) was determined immunologically in the cell extracts, wash (W1, W6 and W7) and elution fractions (E1 and E2).

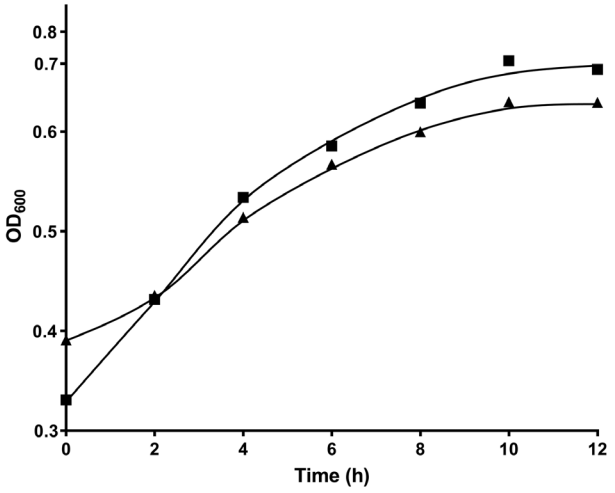

Fig. 7. Growth of the *A. woodii* Δ*adh4* mutant and the Δ*pyrE* strain on 1,2-PD. *Acetobacterium woodii* Δ*pyrE* (■) and Δ*adh4* (▲) were first grown on complex media supplemented with 100 mM sodium formate to an OD_{600} = ~0.35. To the same culture, 1,2-PD (15 mM) was added at time point zero. Growth was monitored for the next 12 h. Each data point is representative of three biological replicates.

dehydrogenase) deletion mutant in *S. enterica* was reported earlier (Cheng *et al*., 2012).

Further, we tested whether the Δ*adh4* mutant also displayed similar growth defects during growth on BMC-forming substrates like ethanol (50 mM) or 2,3-BD (20 mM). Therefore, the Δ*adh4* mutant and Δ*pyrE* strain were adapted and grown on the respective substrates. Growth was monitored and doubling time of both these strains were recorded. Compared to Δ*pyrE*, the Δ*adh4* mutant displayed only 13% and 10% prolonged doubling time when grown on ethanol or 2,3-BD respectively (data not shown). Apparently, deletion of *adh4* in *A. woodii* did not severely affect growth on ethanol or 2,3-BD as was observed on 1,2-PD.

Δadh4 *mutant produced less propanol during growth on 1,2-propanediol*

Further, to show that Adh4 is involved in the metabolism of 1,2-PD, we analysed the product pool of the mutant strains during growth on 1,2-PD. As evident from Fig. 8, 1,2-PD was completely consumed within 12 h by both, the Δ*pyrE* and Δ*adh4* mutant and propionate and propanol were formed as end products. As expected, Δ*pyrE* cells produced equimolar amounts of propanol and propionate (7.3 mM versus 8 mM) from 1,2-PD (15 mM). Strikingly, the Δ*adh4* mutant produced much less propanol compared to propionate (3.5 mM versus 13.6 mM). Though the consumption rate of 1,2-PD was similar for the Δ*pyrE* and Δ*adh4* mutant (3.9 mM/h versus 4 mM/h), the rate of propanol formation was markedly lower in the Δ*adh4* mutant (1.1 mM/h versus 0.3 mM/h). While the results for the Δ*pyrE* are in agreement with the stoichiometry of the fermentation balance: 1,2-propanediol → 0.5 propanol +0.5 propionate, the ratio of propionate to propanol formation was found to be 4:1 in the Δ*adh4* mutant. Apparently, deletion of *adh4* disbalances the propionaldehyde to propanol pathway with a shift towards the formation of propionate.

Resting cell experiments with Δadh4 *mutant*

The stoichiometry of propanol and propionate formation from 1,2-PD was analysed in resting cells since carbon is not utilized for biomass production. Therefore the Δ*pyrE* and Δ*adh4* mutant were grown on 1,2-PD as described above and harvested until no further change in OD_{600} was observed. The cells were washed two times, resuspended in 10 ml of reaction buffer with a total protein concentration adjusted to 1 mg ml^{-1}. 1,2-PD was added to the cell suspension at time point zero (t_0) to a concentration of 15 mM. As shown in Fig. 9, 1,2-PD (15 mM) was rapidly degraded and completely consumed within 15 min by both the Δ*pyrE* and Δ*adh4* mutant. At the same time, at least 10 mM propionaldehyde appeared in the medium, which was then completely consumed in the next 135 min. In the Δ*pyrE* cells, the products propanol and propionate were formed in equimolar amounts (7.1 mM versus 7.5 mM) with a rate of 0.34 μmol min^{-1} mg^{-1} each. Interestingly, the same was not true for the Δ*adh4* mutant. Though propionaldehyde was consumed at a similar rate (0.10 μmol min^{-1} mg^{-1}) as in the Δ*pyrE* strain (0.11 μmol min^{-1} mg^{-1}), the rate of formation of propionate was much faster (0.5 μmol min^{-1} mg^{-1}) but propanol formation was much slower (0.20 μmol min^{-1} mg^{-1}). As is evident from Fig. 9, the final concentration of propionate formed (10.7 mM) was more than the double of propanol formed (4.4 mM). Apparently, the Δ*adh4* mutant produced 0.9 mM of acetate compared to 0.1 mM by the Δ*pyrE* strain indicating that electrons are re-directed into the WLP.

Discussion

Bacterial microcompartments are essential for optimizing segments of metabolic pathways and also to encapsulate toxic intermediates (acetaldehyde or propionaldehyde) to reduce cytotoxicity (Cheng *et al*., 2008; Kerfeld *et al*., 2010; Jorda *et al*., 2013; Chowdhury *et al*., 2014). While BMCs are produced by various classes of bacteria in form of carboxysomes or metabolosomes, the acetogen *A. woodii* has recently been described to utilize BMCs for a non-acetogenic mode of life (Schuchmann *et al*., 2015). *Acetobacterium woodii* grows on 1,2-PD as a sole carbon and energy source to produce propionate

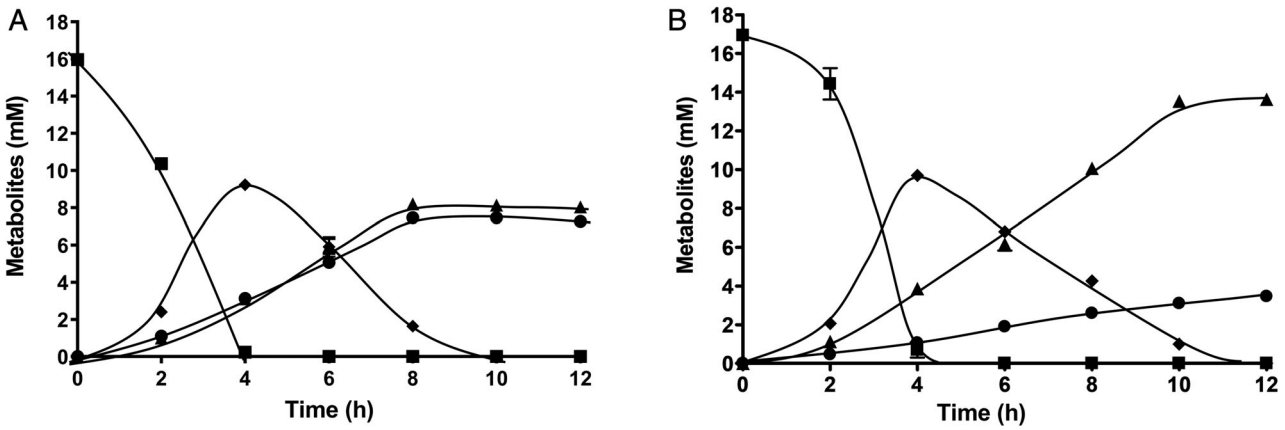

Fig. 8. Products formed from 1,2-PD by the Δ*adh4* and Δ*pyrE* mutant. *Acetobacterium woodii* Δ*pyrE* (A) and Δ*adh4* (B) were grown as described in Fig. 7. Samples were drawn at different time points during growth and concentration of 1,2-PD (■), propionaldehyde (♦), propanol (●) and propionate (▲) was analysed by gas chromatography.

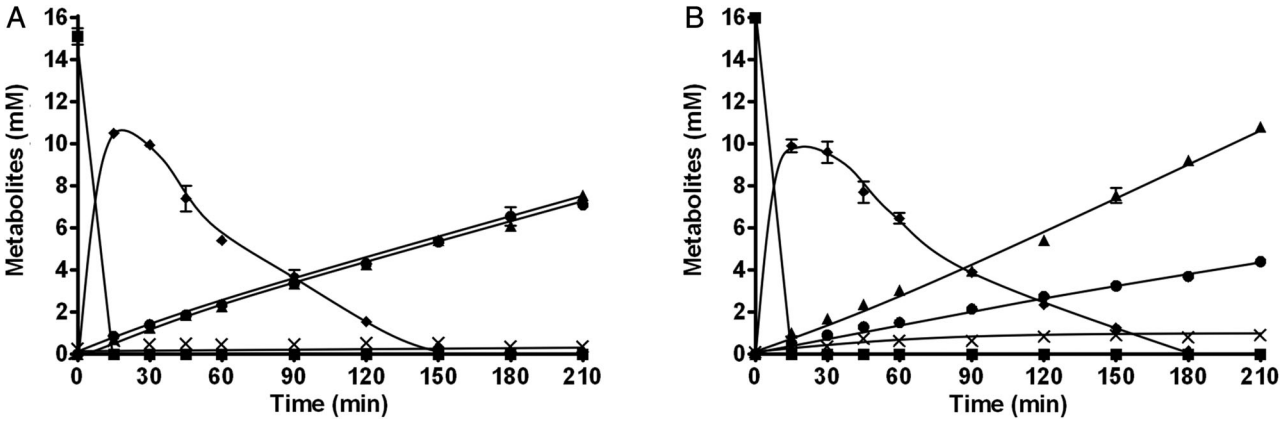

Fig. 9. Conversion of 1,2-PD by resting cells of *A. woodii* Δ*pyrE* and Δ*adh4*. *Acetobacterium woodii* Δ*pyrE* (A) and Δ*adh4* (B) mutant strains were grown on 1,2-PD as described in Fig. 7, harvested, washed twice and resuspended to a final protein concentration of 1 mg ml^{-1} in 10 ml buffer in 115-ml serum bottles under a N_2/CO_2 atmosphere (80:20 [vol/vol]). Samples were drawn at different time points for quantification of 1,2-PD (■), propionaldehyde (♦), propanol (●) propionate (▲) and acetate (×) by gas chromatography. All experiments were performed in duplicates.

and propanol as metabolic end products and it is speculated that *A. woodii* produces BMCs during growth on diols and ethanol to encase toxic aldehyde intermediates generated during metabolism, as suggested for *Salmonella* (Sampson and Bobik, 2008). In *A. woodii*, aldehyde detoxification occurs in a bifurcated manner by two concomitant parallel enzymatic steps; in one direction by coenzyme A-dependent oxidation of aldehyde to its corresponding CoA thioester (propionyl-CoA) by CoA-dependent propanediol dehydrogenase (PduP) and on the other by reduction of aldehyde to its corresponding alcohol (propanol) by an uncharacterized alcohol dehydrogenase.

Existing knowledge of 1,2-PD metabolism by other organisms like *Salmonella enterica* established that the 1-propanol dehydrogenase (*pduQ*) is solely responsible for reduction of propionaldehyde to propanol and also for internal recycling of NAD^+ (Cheng *et al*., 2012). In this study, we demonstrated that during growth of *A. woodii* on 1,2-PD and 2,3-BD as sole carbon source, among 11 alcohol dehydrogenases encoded in the genome, two putative alcohol dehydrogenase genes, *adh4* and *adh6* were highly transcribed. While both gene products (Adh4 and Adh6) reduced propionaldehyde, Adh4 was by far much more active than Adh6. The finding that Adh4 co-purified with the intact *A. woodii* BMC and also during *in vivo* pull-down assays using His_6-PduB as a bait, indicated that Adh4 is indeed an integral component of *A. woodii* BMCs. Adh4 exhibited high propionaldehyde reduction activity (~150 μmol min^{-1} mg^{-1}) with low propanol oxidation activity (0.63 μmol min^{-1} mg^{-1}), clearly indicating that the forward reaction towards propanol formation is favoured by the enzyme. While it is absolutely essential that at least one alcohol

dehydrogenase is present along with the PduP enzyme within the BMC for NAD^+ recycling, this does not rule out the presence of a second alcohol dehydrogenase within the BMCs. *Acetobacterium woodii* grows on a variety of substrates like 2,3-BD, ethanol, ethylene glycol or 1,2-PD, which are individually metabolized utilizing different pathways and also involving multiple different alcohol dehydrogenases. Despite the difference of the substrates, BMCs are always produced. Therefore, it is also possible that a second alcohol dehydrogenase is present within the BMCs and plays an equally important role in reduction of aldehyde to its corresponding alcohol. While it has been reported that trafficking of internal enzymes into the BMCs is accomplished by encapsulation peptides generally located at the N- or C-terminus of each enzyme, such an encapsulation peptide could not be identified at the C-terminal end of BMC-associated alcohol dehydrogenase (Aussignargues *et al*., 2015). However, on closer inspection of the N- and the C-termini of both Adh4 and Adh6, a short peptide ($\sim$ 12 aa) at the C-terminus, predicted to fold as an alpha-helix could be identified (See Fig. S4) using the JPred server (Cole *et al*., 2008). A similar short peptide sequence was also identified at the C-terminal end of PduQ, but the predicted alpha-helix fold does not fit the definition of an encapsulation peptide (no apparent amphipathicity of the helix) (Kinney *et al*., 2012). Moreover, it has been shown that PduQ forms a complex with PduP suggesting it may be encapsulated by piggy-banking (Cheng *et al*., 2012). In *A. woodii*, it is likely that the alcohol dehydrogenase Adh4 co-localizes within the BMCs by protein–protein interaction with PduB as revealed by pull-down experiments.

Though not being a part of the *pdu* cluster, deletion of the a*dh4* gene indeed resulted in a slow growth phenotype compared to the Δ*pyrE* strain when grown on 1,2-PD as carbon source. Theoretically, at the end of 1,2-PD metabolism by *A. woodii*, equimolar amounts of propionate and propanol should be formed as metabolic end products from metabolism of 15 mM 1,2-PD. Indeed, this was true in case of the Δ*pyrE* strain but not in the Δ*adh4* mutant that produced a much higher amount of propionate compared to propanol. In absence of Adh4, propionaldehyde reduction was severely impaired whereby the extra propionaldehyde (carbon) flux was pushed towards the formation of propionate. One would expect that on impairment of the NAD^+ regeneration pathway, the mutant cells would exhibit a severe growth phenotype. In this case, our experimental results suggested that *A. woodii* has another alcohol dehydrogenase, which allowed NAD^+ recycling with propanol formation albeit with much lower activity. Low concentrations of propanol could also be formed by Adh6, which was found to be highly expressed during growth on 1,2-PD or any other alcohol dehydrogenase that might be activated by deletion of *adh4*. It is possible that another alcohol dehydrogenase is either imported within the BMC or propionaldehyde traverses outside the BMC to be reduced to propanol for NAD^+ regeneration. In either of the case, in the Δ*adh4* mutant, this turns out to be less efficient. It is clear that Adh4 is required for a complete functional BMC and that its removal causes imbalance in 1,2-PD metabolism.

Furthermore, one question arises: how is the excess NADH reoxidized in the *adh4* mutant? It is likely that NADH is reoxidized in the Wood-Ljungdahl pathway, which is consistent with the observed production of acetate. How this is achieved remains open but it shows a complex electron-balancing between acetogenic and non-acetogenic lifestyle. In summary, in this study we could identify, characterize and illustrate the localization of the missing BMC-associated-alcohol dehydrogenase in *A. woodii*. We have successfully assigned function to one of the 11 alcohol dehydrogenases involved in propanol formation. This study also broadens our knowledge and understanding how metabolic modules involving BMCs are controlled in an ancient organism along with other energy conserving processes like chemiosmosis and ATP hydrolysis.

Experimental procedures

Growth of A. woodii

Acetobacterium woodii DSMZ 1030 and mutants were cultivated under strictly anoxic conditions at 30°C in carbonate buffered complex media as described previously (Heise *et al*., 1989). Fructose (20 mM), 1,2-propanediol (15 mM), 2,3-butanediol (20 mM) or ethylene-glycol (20 mM) served as carbon and energy source unless otherwise mentioned. For growth studies on 1,2-propanediol (1,2-PD), *A. woodii* strains (Δ*pyrE* and Δ*adh4*) were first grown on 100 mM sodium formate. At stationary phase when all carbon (formate) was consumed, 1,2-PD was given to a final concentration of 15 mM as described previously (Chowdhury *et al*., 2020). Growth was monitored by measuring the optical density at 600 nm. The growth experiments were performed in 115-ml serum flasks containing 50 ml of media.

Quantitative PCR (qRTPCR) analysis. RNA was prepared from *A. woodii* cells grown on 1,2-PD, 2,3-BD or ethylene glycol to mid-exponential growth phase as described earlier (Chowdhury *et al*., 2020). 1 μg of RNA from each sample was converted into cDNA by using M-MLV Reverse Transcriptase according to the manufacturer's protocol (Promega, Mannheim, Germany). All quantitative PCRs were performed in triplicate, using

Ssofast Evagreen Supermix (Bio-Rad, CA, USA) with 1 ng cDNA as template and 500 nM of gene specific primers in a final reaction volume of 25 μl. Transcript levels of *adh1*, *adh4* and *adh6* were analysed using gene specific primers (Table S1). Transcript levels of all the genes tested were normalized to transcript levels of the gene *gyrA* as described previously (Chowdhury *et al*., 2020).

Cloning and overproduction of Adh4 and Adh6

The genes encoding Adh4 (Awo_c06220) and Adh6 (Awo_c25410) were amplified from chromosomal DNA of *A. woodii* with gene specific primer (Table S1). The PCR products were cloned into pET-21a (+) vector and the resulting plasmids were transformed into *E. coli* BL-21 (DE3) for overproduction of the H_6- tagged_Adh4 or Adh6 proteins. The transformants were grown at 37°C in LB medium to an OD_{600} of 0.6–0.8 and gene expression was induced by addition of Isopropyl-D-galactopyranoside (IPTG) to a final concentration of 1 mM. After incubation at 16°C for 16 h, cells were harvested by centrifugation and disrupted by passage through a French press (SLM Instruments, United States) at 100 MPa. Proteins were purified using 6X-histidine tag from the cell lysates under strictly anoxic conditions using buffer A (50 mM sodium phosphate buffer, pH 8.0, 300 mM NaCl) containing 250 mM imidazole. The protein purity was analysed on a 12% denaturing SDS-polyacrylamide gel (Laemmli, 1970) and further staining with Coomassie brilliant blue G250 (Meyer and Lambert, 1965).

Measurement of enzymatic activities

All enzymatic assays were performed with His_6-tagged Adh4 or Adh6. Measurements were carried out in 1 ml of anoxic buffer in 1.8 ml sealed cuvettes with a gas phase of 100% N_2. The activities of Adh4 and Adh6 were measured by propionaldehyde-dependent oxidation of NADH at 340 nm with 10 μg of purified proteins in a 50 mM Tris–HCl buffer (pH 7.5) containing 50 mM NaCl, 2 mM DTE, 250 μM NADH and 50 mM propionaldehyde. The reverse reaction (1-propanol oxidation) was measured in a 25 mM CHES buffer (pH 9.0), 0.6 mM NAD^+ and 400 mM 1-propanol. The increase of NADH concentration was monitored at 340 nm ($\varepsilon = 6.3\ mM^{-1}\ cm^{-1}$) (Ziegenhorn *et al*., 1976). For the determination of V_{max} and K_m values, the data were fitted by non-linear curve fitting using GraphPad Prism 5.01 Software (GraphPad Software, San Diego, CA).

Antibody generation and analytical method

Concentration of purified proteins was measured according to Bradford (Bradford, 1976). For generation of Adh4 antibody, Adh4-His_6 protein (see above) was separated and analysed by SDS-PAGE and visualized by staining with Coomassie brilliant blue G250 (Sigma-Aldrich Chemie GmbH). Adh4 was cut from a Coomassie-stained SDS gel and used to immunize rabbits. Antisera prepared from immunized rabbits were used for blotting purpose. Other antibodies against PduB, PduT, PduP and PduC proteins were used as described earlier (Schuchmann *et al*., 2015). For immunological detection of BMC associated proteins, purified BMC fractions (10–20 μg) were separated on 12% polyacrylamide gels. Proteins were transferred on to a nitrocellulose membrane (Protran BA 83; GE Healthcare, United Kingdom) followed by immunoblotting with a 1:10,000 dilution of the rabbit antiserum antibodies as earlier described (Hess *et al*., 2011).

Pull down assays

BMCs were routinely prepared from *A. woodii* cells grown on 1,2-PD or 2,3-BD as earlier described (Chowdhury *et al*., 2020). For homologous production of PduB and pull-down assay in *A. woodii*, the plasmid (291bpUp_pMTL82254_CAT) was used as a backbone (Chowdhury *et al*., 2020). The *pduB* gene including a DNA sequence at the 3′-end that encodes a 6X-histidine-tag was amplified using *A. woodii* genomic DNA as a template and cloned in to the 291bpUp_pMTL82254_CAT plasmid between the *NdeI* and *NcoI* restrictions sites. In the resulting plasmid, the *catP* gene was replaced by *pduB*, allowing the *pduB* gene to be directly under the control of *pdu* promoter (291 bp). The plasmid was named 291bpUP_pMTL82254_PduB_His. Transformation was performed according to earlier described procedure (Westphal *et al*., 2018). The transformants were grown in volume of 2 l of carbonate buffered media (Heise *et al*., 1989) containing 20 mM 2,3-BD and 15 $\mu g\ ml^{-1}$ erythromycin, as 2,3-BD strongly induced the *pdu* promoter resulting in native-production of His_6-PduB (Chowdhury *et al*., 2020). On reaching the stationary growth phase, cells were harvested by centrifugation and disrupted by passage through a French press (SLM Instruments, United States) at 100 MPa. Cell debris was removed by centrifugation at 17,000 × *g* for 20 min at 4°C. The supernatant was applied on a 2 ml of nickel-nitrilotriacetic acid (Ni-NTA) column, which was equilibrated with buffer A. The histidine tagged PduB was eluted with two column volumes of 250 mM imidazole in buffer A. The purified His_6-PduB and its interacting proteins were analysed using PAGE and further by western blotting.

Generation of A. woodii Δadh4 *strain.* The deletion of *adh4* was made in a *A. woodii pyrE* mutant for counter selective purpose (Wiechmann *et al*., 2020). The resulting strain is isogenic to the *pyrE* mutant except for

the *adh4* deletion. For deletion of *adh4*, a plasmid pMTL84151_JM_dadh4 was constructed. Therefore, the *adh4* deletion cassette was cloned in the multiple cloning site (MCS) of the background plasmid pMTL84151 (Heap *et al*., 2007), consisting of 1000 bp of upstream- and downstream flanking regions of *adh4* (Awo_c06220), which enables the deletion of *adh4 via* homologous recombination. The constructed plasmid lacks a replicon for Gram positive bacteria and possesses a gene encoding for thiamphenicol resistance from *Clostridium perfringens* (Werner *et al*., 1977) and a heterologous *pyrE* gene cassette from *Clostridium acetobutylicum* as a counter selectable marker. Plasmid transformation into the *A. woodii pyrE* mutant and further integration and recombination of the *adh4* deletion cassette was performed as described (Westphal *et al*., 2018). The deletion the *adh4* gene was verified by amplifying the flanking regions and further by DNA sequencing analysis.

Preparation of cell suspensions and analysis

For cell suspension analysis, Δ*pyrE* and Δ*adh4* strains were grown as described earlier until no further change in OD_{600} was observed, harvested by centrifugation (10,000 × g; 10 min) and washed two times with imidazole buffer A (50 mM imidazole-HCl, 20 mM MgSO4, 20 mM KCl, 2 mM dithioerythritol (DTE), 1 mg litre^{-1} resazurin, pH 7.0) under strictly anoxic conditions in an anaerobic chamber (Coy Laboratory Products, Grass Lake, MI) filled with 95% to 98% N_2 and 2% to 5% H_2 as described previously (Heise *et al*., 1992). The protein concentration of the cell suspension was determined as described previously (Schmidt *et al*., 1963). Cells were resuspended in 115-ml glass bottles in resuspension buffer (imidazole buffer supplemented with 20 mM NaCl and 60 mM $KHCO_3$, pH 7.2) under a N_2/CO_2 atmosphere (80:20 [vol/vol]) such that the total protein concentration was 1 mg/ml in a volume of 10 ml. The suspensions were incubated at 30°C in a shaking water bath. Substrate/product analysis were done from 500 µl samples withdrawn with a syringe at different time points. The concentrations of 1,2-PD, 1-propanol, propionate and acetate were determined by gas chromatography as described previously (Schuchmann *et al*., 2015). The peak areas were proportional to the concentration of each substance and calibrated with standard curves. A total of 5 mM butanol was used as the internal standard for all measurements.

Acknowledgements

The research was funded by an Advanced Grant of the European Research Council under the European Union's Horizon 2020 Research and Innovation Program (grant agreement no. 741791).

References

Aussignargues, C., Paasch, B.C., Gonzalez-Esquer, R., Erbilgin, O., and Kerfeld, C.A. (2015) Bacterial microcompartment assembly: the key role of encapsulation peptides. *Commun Integr Biol* **8**: e1039755.

Axen, S.D., Erbilgin, O., and Kerfeld, C.A. (2014) A taxonomy of bacterial microcompartment loci constructed by a novel scoring method. *PLoS Comput Biol* **10**: e1003898.

Bertsch, J., Siemund, A.L., Kremp, F., and Müller, V. (2016) A novel route for ethanol oxidation in the acetogenic bacterium *Acetobacterium woodii*: the acetaldehyde/ethanol dehydrogenase pathway. *Environ Microbiol* **18**: 2913–2922.

Blackwell, C.M., and Turner, J.M. (1978) Microbial metabolism of amino alcohols. Purification and properties of coenzyme B12-dependent ethanolamine ammonia-lyase of *Escherichia coli*. *Biochem J* **175**: 555–563.

Bobik, T.A., Havemann, G.D., Busch, R.J., Williams, D.S., and Aldrich, H.C. (1999) The propanediol utilization (pdu) operon of *Salmonella enterica* serovar Typhimurium LT2 includes genes necessary for formation of polyhedral organelles involved in coenzyme B(12)-dependent 1, 2-propanediol degradation. *J Bacteriol* **181**: 5967–5975.

Bobik, T.A., Xu, Y., Jeter, R.M., Otto, K.E., and Roth, J.R. (1997) Propanediol utilization genes (*pdu*) of *Salmonella typhimurium*: three genes for the propanediol dehydratase. *J Bacteriol* **179**: 6633–6639.

Bradford, M.M. (1976) A rapid and sensitive method for the quantification of microgram quantities of protein utilizing the principle of proteine-dye-binding. *Anal Biochem* **72**: 248–254.

Cheng, S., Fan, C., Sinha, S., and Bobik, T.A. (2012) The PduQ enzyme is an alcohol dehydrogenase used to recycle NAD^+ internally within the Pdu microcompartment of *Salmonella enterica*. *PLoS One* **7**: e47144.

Cheng, S., Liu, Y., Crowley, C.S., Yeates, T.O., and Bobik, T.A. (2008) Bacterial microcompartments: their properties and paradoxes. *Bioessays* **30**: 1084–1095.

Chowdhury, C., Sinha, S., Chun, S., Yeates, T.O., and Bobik, T.A. (2014) Diverse bacterial microcompartment organelles. *Microbiol Mol Biol Rev* **78**: 438–468.

Chowdhury, N.P., Alberti, L., Linder, M., and Müller, V. (2020) Exploring bacterial microcompartments in the acetogenic bacterium *Acetobacterium woodii*. *Front Microbiol* **11**: 593467.

Cole, C., Barber, J.D., and Barton, G.J. (2008) The Jpred 3 secondary structure prediction server. *Nucleic Acids Res* **36**: W197–W201.

Drake, H.L. (1994) Acetogenesis, acetogenic bacteria, and the acetyl-CoA "Wood/Ljungdahl" pathway: past and current perspectives. In *Acetogenesis*, Drake, H.L. (ed). New York, NY: Springer, pp. 3–60.

Drake, H.L., Daniel, S., Küsel, K., Matthies, C., Kuhner, C., and Braus-Strohmeyer, S. (1997) Acetogenic bacteria: what are the *in situ* consequences of their diverse metabolic diversities? *Biofactors* **1**: 13–24.

Havemann, G.D., Sampson, E.M., and Bobik, T.A. (2002) PduA is a shell protein of polyhedral organelles involved in coenzyme B(12)-dependent degradation of 1,2-propanediol in *Salmonella enterica* serovar typhimurium LT2. *J Bacteriol* **184**: 1253–1261.

Heap, J.T., Pennington, O.J., Cartman, S.T., Carter, G.P., and Minton, N.P. (2007) The ClosTron: a universal gene knock-out system for the genus *Clostridium*. *J Microbiol Methods* **70**: 452–464.

Heise, R., Müller, V., and Gottschalk, G. (1989) Sodium dependence of acetate formation by the acetogenic bacterium *Acetobacterium woodii*. *J Bacteriol* **171**: 5473–5478.

Heise, R., Müller, V., and Gottschalk, G. (1992) Presence of a sodium-translocating ATPase in membrane vesicles of the homoacetogenic bacterium *Acetobacterium woodii*. *Eur J Biochem* **206**: 553–557.

Hess, V., Oyrik, O., Trifunovic, D., and Müller, V. (2015) 2,3-butanediol metabolism in the acetogen *Acetobacterium woodii*. *Appl Environ Microbiol* **81**: 4711–4719.

Hess, V., Vitt, S., and Müller, V. (2011) A caffeyl-coenzyme A synthetase initiates caffeate activation prior to caffeate reduction in the acetogenic bacterium *Acetobacterium woodii*. *J Bacteriol* **193**: 971–978.

Jorda, J., Lopez, D., Wheatley, N.M., and Yeates, T.O. (2013) Using comparative genomics to uncover new kinds of protein-based metabolic organelles in bacteria. *Protein Sci* **22**: 179–195.

Kerfeld, C.A., Heinhorst, S., and Cannon, G.C. (2010) Bacterial microcompartments. *Annu Rev Microbiol* **64**: 391–408.

Kerfeld, C.A., Sawaya, M.R., Tanaka, S., Nguyen, C.V., Phillips, M., Beeby, M., and Yeates, T.O. (2005) Protein structures forming the shell of primitive bacterial organelles. *Science* **309**: 936–938.

Kinney, J.N., Salmeen, A., Cai, F., and Kerfeld, C.A. (2012) Elucidating essential role of conserved carboxysomal protein CcmN reveals common feature of bacterial microcompartment assembly. *J Biol Chem* **287**: 17729–17736.

Klein, M.G., Zwart, P., Bagby, S.C., Cai, F., Chisholm, S.W., Heinhorst, S., *et al*. (2009) Identification and structural analysis of a novel carboxysome shell protein with implications for metabolite transport. *J Mol Biol* **392**: 319–333.

Kofoid, E., Rappleye, C., Stojiljkovic, I., and Roth, J. (1999) The 17-gene ethanolamine (eut) operon of *Salmonella typhimurium* encodes five homologues of carboxysome shell proteins. *J Bacteriol* **181**: 5317–5329.

Laemmli, U.K. (1970) Cleavage of structural proteins during the assembly of the head of bacteriophage T4. *Nature* **227**: 680–685.

Ljungdahl, L.G. (1969) Total synthesis of acetate from CO_2 by heterotrophic bacteria. *Annu Rev Microbiol* **23**: 515–538.

Meyer, T., and Lambert, T. (1965) Use of coomassie brilliant blue R250 for the electrophoresis of microgram quantities of parotid saliva proteins on acrylamide-gel strips. *Biochim Biophys Acta* **107**: 144–145.

Müller, V. (2003) Energy conservation in acetogenic bacteria. *Appl Environ Microbiol* **69**: 6345–6353.

Penrod, J.T., and Roth, J.R. (2006) Conserving a volatile metabolite: a role for carboxysome-like organelles in *Salmonella enterica*. *J Bacteriol* **188**: 2865–2874.

Poehlein, A., Schmidt, S., Kaster, A.-K., Goenrich, M., Vollmers, J., Thürmer, A., *et al*. (2012) An ancient pathway combining carbon dioxide fixation with the generation and utilization of a sodium ion gradient for ATP synthesis. *PLoS One* **7**: e33439.

Ragsdale, S.W., and Wood, H.G. (1985) Acetate biosynthesis by acetogenic bacteria. Evidence that carbon monoxide dehydrogenase is the condensing enzyme that catalyzes the final steps in the synthesis. *J Biol Chem* **260**: 3970–3977.

Reid, M.F., and Fewson, C.A. (1994) Molecular characterization of microbial alcohol dehydrogenases. *Crit Rev Microbiol* **20**: 13–56.

Rondon, M.R., and Escalante-Semerena, J.C. (1992) The poc locus is required for 1,2-propanediol-dependent transcription of the cobalamin biosynthetic (cob) and propanediol utilization (pdu) genes of *Salmonella typhimurium*. *J Bacteriol* **174**: 2267–2272.

Sampson, E.M., and Bobik, T.A. (2008) Microcompartments for B12-dependent 1,2-propanediol degradation provide protection from DNA and cellular damage by a reactive metabolic intermediate. *J Bacteriol* **190**: 2966–2971.

Schmidt, K., Liaaen-Jensen, S., and Schlegel, H.G. (1963) Die Carotinoide der *Thiorhodaceae*. *Arch Mikrobiol* **46**: 117–126.

Schuchmann, K., and Müller, V. (2016) Energetics and application of heterotrophy in acetogenic bacteria. *Appl Environ Microbiol* **82**: 4056–4069.

Schuchmann, K., Schmidt, S., Martinez Lopez, A., Kaberline, C., Kuhns, M., Lorenzen, W., *et al*. (2015) Nonacetogenic growth of the acetogen *Acetobacterium woodii* on 1,2-propanediol. *J Bacteriol* **197**: 382–391.

Shively, J.M., Ball, F., Brown, D.H., and Saunders, R.E. (1973) Functional organelles in prokaryotes: polyhedral inclusions (carboxysomes) of *Thiobacillus neapolitanus*. *Science* **182**: 584–586.

Shively, J.M., English, R.S., Baker, S.H., and Cannon, G.C. (2001) Carbon cycling: the prokaryotic contribution. *Curr Opin Microbiol* **4**: 301–306.

Toraya, T., Honda, S., and Fukui, S. (1979) Fermentation of 1,2-propanediol with 1,2-ethanediol by some genera of Enterobacteriaceae, involving coenzyme B12-dependent diol dehydratase. *J Bacteriol* **139**: 39–47.

Trifunovic, D., Berghaus, N., and Müller, V. (2020) Growth of the acetogenic bacterium *Acetobacterium woodii* by dismutation of acetaldehyde to acetate and ethanol. *Environ Microbiol Rep* **12**: 58–62.

Trifunović, D., Schuchmann, K., and Müller, V. (2016) Ethylene glycol metabolism in the acetogen *Acetobacterium woodii*. *J Bacteriol* **198**: 1058–1065.

Werner, H., Krasemann, C., Gorniak, W., Hermann, A., and Ungerechts, J. (1977) Susceptibility to thiamphenicol and chloramphenicol of anaerobic bacteria. *Zentralbl Bakteriol Orig A* **237**: 358–371.

Westphal, L., Wiechmann, A., Baker, J., Minton, N.P., and Müller, V. (2018) The Rnf complex is an energy coupled transhydrogenase essential to reversibly link cellular NADH and ferredoxin pools in the acetogen *Acetobacterium woodii*. *J Bacteriol* **200**: e00357–e00318.

Wiechmann, A., Ciurus, S., Oswald, F., Seiler, V.N., and Müller, V. (2020) It does not always take two to tango:

"Syntrophy" via hydrogen cycling in one bacterial cell. *ISME J* **14**: 1561–1570.

Wood, H.G., and Ljungdahl, L.G. (1991) Autotrophic character of the acetogenic bacteria. In *Variations in Autotrophic Life*, Shively, J.M., and Barton, L.L. (eds). San Diego, CA: Academic press, pp. 201–250.

Ziegenhorn, J., Senn, M., and Bucher, T. (1976) Molar absorptivities of beta-NADH and beta-NADPH. *Clin Chem* **22**: 151–160.

Supporting Information

Additional Supporting Information may be found in the online version of this article at the publisher's web-site:

Fig. S1. Dependence of Adh4 activity on the concentration of butyraldehyde (A) or acetaldehyde (B). Assays were performed with 10 μg of purified proteins in a 50 mM Tris-HCl buffer (pH 7.5) containing 50 mM NaCl, 2 mM DTE, 250 μM NADH and the indicated concentrations of butyraldehyde or acetaldehyde. Activity was measured by respective aldehyde-dependent oxidation of NADH at 340 nm. Curve fitting and determination of the kinetic parameters K_m and V_{max} were performed using the GraphPad Prism program (version 5).

Fig. S2. pH (A) and temperature (B) dependence of propionaldehyde reduction catalyzed by Adh4. Measurement was carried out in 1 ml of anoxic buffer in 1.8 ml sealed cuvettes with gas phase of 100% N_2. Adh4 activity was measured by propionaldehyde-dependent oxidation of NADH at 340 nm. For pH optima, combined buffer mix of 25 mM each MES, MOPS, Tris and CHES with different pH values as indicated was used. For temperature optima measurement, assays were performed in Tris-HCl buffer (pH 7.5) at variable temperature as depicted. Each assay contained 10 μg of Adh4 enzyme, 2 mM DTE, 250 μM NADH and 50 mM propionaldehyde.

Fig. S3. 1-propanol-dependent reduction of NAD^+ catalyzed by Adh4. Measurement was carried out in 1 ml of anoxic buffer in 1.8 ml sealed cuvettes with gas phase of 100% N_2. 1-propanol oxidation was measured in a buffer mix of 25 mM each MES, MOPS, Tris, CHES (pH 9.0). Each assay contained 40 μg of enzyme, 400 mM 1-propanol and different concentrations of NAD^+. The increase in NADH concentration was monitored at 340 nm (ε = 6.3 $mM^{-1}cm^{-1}$). Curve fitting and determination of the kinetic parameters K_m and V_{max} were performed using the GraphPad Prism program (version 5).

Fig. S4. Encapsulation peptide prediction of Adh4 and Adh6. Encapsulation peptides (EPs) are characterized by a primary structure predicted to form an amphipathic α-helix. Secondary structure of the N- and C-terminal ends of Adh4, Adh6 of *A. woodii* and PduQ of *S. enterica* was predicted using the JPred server. For secondary structure prediction, 30 aa from either N- or C-terminal end of each protein were analysed. Helix region is highlighted in *grey*.

Table S1. Primers used in this study.